

# Pattern dynamics and spatiotemporal chaos in the quantum Zakharov equations

A. P. Misra\*

*Department of Mathematics, Visva-Bharati University, Santiniketan 731 235, India*

P. K. Shukla†

*Institut für Theoretische Physik IV and Centre for Plasma Science and Astrophysics, Fakultät für Physik and Astronomie, Ruhr-Universität Bochum, D-44780 Bochum, Germany*

(Received 23 January 2009; published 4 May 2009)

The dynamical behavior of the nonlinear interaction of quantum Langmuir waves (QLWs) and quantum ion-acoustic waves (QIAWs) is studied in the one-dimensional quantum Zakharov equations. Numerical simulations of coupled QLWs and QIAWs reveal that many coherent solitary patterns can be excited and saturated via the modulational instability of unstable harmonic modes excited by a modulation wave number of monoenergetic QLWs. The evolution of such solitary patterns may undergo the states of spatially partial coherence (SPC), coexistence of temporal chaos and spatiotemporal chaos (STC), as well as STC. The SPC state is essentially due to ion-acoustic wave emission and due to quantum diffraction, while the STC is caused by the combined effects of SPC and quantum diffraction, as well as by collisions and fusions among patterns in stochastic motion. The energy in the system is strongly redistributed, which may switch on the onset of weak turbulence in dense quantum plasmas.

DOI: [10.1103/PhysRevE.79.056401](https://doi.org/10.1103/PhysRevE.79.056401)

PACS number(s): 52.25.Gj, 52.35.Mw, 05.45.Mt

## I. INTRODUCTION

Quantum plasma phenomena are relevant in ultrasmall electronic devices and micromechanical systems [1], in dense laser-plasmas and microplasmas [2], as well as in dense astrophysical objects [3]. Many collective processes have been investigated in this area (e.g., see Refs. [4–10]). New quantum modes have also been identified for ultracold dusty plasmas (see, e.g., Refs. [11–16]). The recent developments include the spin effects [17–19] in nonrelativistic quantum plasmas, as well as in the associated magnetohydrodynamic equations [20], with possible important applications to solid density plasmas, as well as in the vicinity of pulsars and magnetars. In addition, there are new experimental studies [21] of weakly degenerate quantum plasmas in a gaseous regime. The formations of dark solitons as well as quantum vortices are also found in quantum electron plasmas [22]. These nonlinear nanostructures can efficiently transport information over short distances. Furthermore, Dastgeer and Shukla [23,24] studied two- and three-dimensional aspects of electron fluid turbulence at nanoscales. A review on quantum plasma models and their range of validity can be found in Ref. [25].

The quantum Zakharov equations (QZEs) [26], which describe the nonlinear interaction of high-frequency quantum Langmuir and low-frequency quantum ion-acoustic waves, extend the classical Zakharov system [27] to the quantum realm. The QZEs are deduced from a multiple time-scale method applied to a set of quantum hydrodynamic (QHD) equations under quasineutral assumption. Applications can be found for quantum decay and four-wave instabilities, where significant departures from the classical dispersion re-

lations are found [26]. Notice that the QZEs do not reduce, in the adiabatic limit, to a nonlinear Schrödinger equation (NLSE) for the envelope electric field [26]. Rather, the adiabatic limit produces a coupled system for the envelope electric field and the density fluctuation, whose complete integrability is not assured at all. Further developments on the QZEs involve the effects of statistical superpositions of Langmuir waves, where the combined effect of partial coherence and quantum corrections tends to enhance the modulational instability (MI) [28]. The variational formalism on the QZEs is also carried out recently by Haas [29] to investigate its dynamical behaviors. More recently [30], a few mode expansions were used to substitute the primary partial differential equations system by a set of ordinary differential equations for the temporal dynamics [31,32]. This reduced finite-dimensional system was shown to exhibit hyperchaos (more than one positive Lyapunov exponent).

The pattern formation in spatially extended nonequilibrium dynamical systems has become a major frontier area in science [33]. The existence of spatiotemporal chaos (STC) characterized by its extensive incoherent (irregular) pattern dynamics in both space and time significantly enriches the study of pattern formation. STC has been studied numerically and experimentally in many physical systems (see, e.g., Ref. [33]). However, the mechanism leading to STC still remains unclear. Transition to STC-like phenomena with coexisting temporal chaos (TC) and spatially partial coherence (SPC) states form solitary patterns excited by a modulation wave number in classical plasma systems through the MI of a spatially homogeneous background field has been investigated in the past [34,35]. Recently, the evolution of pattern dynamics and STC in the classical conserved Zakharov equations have been studied numerically by He *et al.* [36,37].

The primary goal of this work is to reconsider the QZEs and to investigate the electron quantum tunneling effect (described by the parameter  $H$ ) on the formation of many soli-

\*apmisra@visva-bharati.ac.in

†ps@tp4.rub.de

itary patterns, the existence of SPC state, the coexistence of TC and STC, as well as the state of STC. The combined effects of SPC and electron quantum tunneling, as well as collisions and fusion among solitary patterns, are the main causes of STC.

## II. QUANTUM ZAKHAROV EQUATIONS AND EVOLUTION OF STC

### A. Quantum Zakharov equations

The one-dimensional QZEs read [26]

$$i\frac{\partial E}{\partial t} + \frac{\partial^2 E}{\partial x^2} - H^2 \frac{\partial^4 E}{\partial x^4} = nE, \quad (1)$$

$$\frac{\partial^2 n}{\partial t^2} - \frac{\partial^2 n}{\partial x^2} + H^2 \frac{\partial^4 n}{\partial x^4} = \frac{\partial^2 |E|^2}{\partial x^2}, \quad (2)$$

where  $E=E(x,t)$  is the envelope of the high-frequency Langmuir wave electric field and  $n=n(x,t)$  is the plasma density fluctuation (measured from its equilibrium value). Moreover,  $H=\hbar\omega_i/\kappa_B T_e$  is a parameter expressing the ratio between the phononic energy density and the electron thermal energy density, where  $\hbar$  is the Planck's constant divided by  $2\pi$ ,  $\kappa_B$  is the Boltzmann constant,  $T_e$  is the electron temperature, and  $\omega_i=\sqrt{n_0 e^2/m_i \epsilon_0}$  is the ion plasma frequency with  $n_0$  denoting the constant background plasma number density and  $m_i$  is the ion mass. The electric field  $E$  has been normalized by  $\sqrt{16m_e n_0 k_B T_e/m_e \epsilon_0}$  and the density  $n$  by  $4m_e n_0/m_i$ , where  $m_e$  being the electron mass. The space and time variables are in units of  $(\lambda_e/2)\sqrt{m_i/m_e}$  and  $m_i/2m_e\omega_e$ , where  $\omega_e=\sqrt{n_0 e^2/m_e \epsilon_0}$  is the electron plasma frequency and  $\lambda_e$  is the electron Debye radius. The formal classical limit is obtained for  $H=0$ , yielding the original Zakharov system. For more details on the derivation of the system as well as for sample applications, see Ref. [26]. The classical Zakharov equations have been widely used to study solitons, chaos, and plasma turbulence in many areas of plasma physics (e.g., Refs. [35,38]). It is thus of current interest to investigate the pattern dynamics as well as the transition to STC in QZEs, which may be useful in understanding the onset of electrostatic plasma-wave turbulence in laboratory and astrophysical quantum plasmas.

The linear stability analysis of the perturbation of the form  $\exp(ikx-i\omega t)$  from a spatially homogeneous field  $E_0$  of a monoenergetic Langmuir wave for Eqs. (1) and (2) gives the growth rate of the MI [28] as

$$\gamma = \frac{1}{\sqrt{2}} [\bar{H}k^2 \sqrt{\bar{H}^2 + 8|E_0|^2} - 2\bar{H}^4 k^2 (2 - \bar{H}^2 k^2) - \bar{H}^2 k^2 (1 + \bar{H}^2 k^2)]^{1/2}, \quad (3)$$

where  $\bar{H}=1+H^2 k^2$ . The growth rate tends to be smaller for increasing values of the quantum parameter  $H$  and is maximum at  $H=0$ . Equations (1) and (2) are not completely integrable, however they admit two kinds of fixed points: a center at  $(0,0)$  and a saddle at  $(E_0,0)$ .

### B. Evolution of STC

We numerically solve Eqs. (1) and (2) to investigate the global behaviors and choose the initial condition to add a small spatial inhomogeneity at  $t=0$  on the spatial homogeneous state  $\Psi_0=(\text{Re } E, \text{Im } E, n, \partial_t n)_{t=0}=(E_0, 0, 0, 0)$  as follows [39]:

$$E(x,0) = E_0[1 + \beta \cos(kx)], \quad n(x,0) = -\sqrt{2}E_0 k \beta \cos(kx), \quad (4)$$

such that  $E_0=(k/\sqrt{2})(1+H^2 k^2)$  holds. Here  $E_0$  represents the amplitude of the pump Langmuir wave and  $\beta$  is a constant of the order of  $10^{-3}$  to emphasize that the perturbation is very small. The initial condition corresponds to slightly perturbed plane Langmuir wave solution of the QZEs and ensures that the manifolds in the phase space will locally lie in a saddle subspace. The QZEs (1) and (2) were simulated using a standard fourth-order Runge-Kutta scheme. A relatively large time step ( $dt=0.001$ ) and mesh size ( $dx=0.1$ ) were chosen in an attempt to study the late time large wavelength behavior of Eqs. (1) and (2). The spatial derivatives were approximated with centered second-order difference approximations. For small values of  $H(\leq 0.5)$ , we used the spatial domain  $-100 \leq x \leq 100$  and for the large values of  $H(> 0.5)$ , we used the domain as  $-150 \leq x \leq 150$ .

The master mode  $k$ , where  $0 < k < \sqrt{2}E_0$ , can, in principle, result in the excitation of  $N-1$  unstable harmonic modes where  $N=[\hat{k}^{-1}]$ , with  $\hat{k}=k/\sqrt{2}E_0$ . There may exist many solitary patterns with spatially modulated length  $l_m=L/m$ , where  $m=1$  is for master mode ( $l_1=L=2\pi/k$ ) and  $m=2, 3, \dots, M$  are for the unstable harmonic modes. As a result, the envelope  $E$  can be expressed as

$$E(x,t) = \sum_{m=1}^M E_m(t) \exp(im\hat{k}x) + \sum_{m=M+1}^{\infty} E_m(t) \exp(im\hat{k}x), \quad (5)$$

where the first term on the right side of Eq. (5) comes from the master mode and unstable harmonic modes with  $M < N-1$  being due to pattern selection, whereas the second term is due to the nonlinear interaction.

The profiles of the electric field and the density fluctuations at the end of simulation are shown in Fig. 1 for  $k=0.7$  and  $H=0$ . We observe an excited electric field of the order  $|E| \sim 2.4$  highly correlated with density depletion  $n \sim -6.9$  or  $n/n_0 \sim -0.015$ . It is observed that there exist critical values of  $k$  and  $H$  for which the motion of the coherent solitary patterns is the temporal recurrence (periodic) or the pseudorecurrence (quasiperiodic) when the unstable wave number lies in  $0 < k < 0.9$  for  $H=0$  and that of the solitary pattern is STC when  $k \geq 0.9$  for  $H=0$  and for  $k \geq 0.7$ ,  $H \geq 0.5$ . The motion of the center of the solitarylike patterns whose initial peak is located at  $x = \pm mL$ ,  $m=0, 1, 2, \dots$  exhibits stochastic behavior. The amplitude of the solitary pattern oscillates and its width varies temporarily. The system is in TC and the spatial behavior is of SPC. It has been pointed out that the resonant overlapping may be the cause for the TC [34].

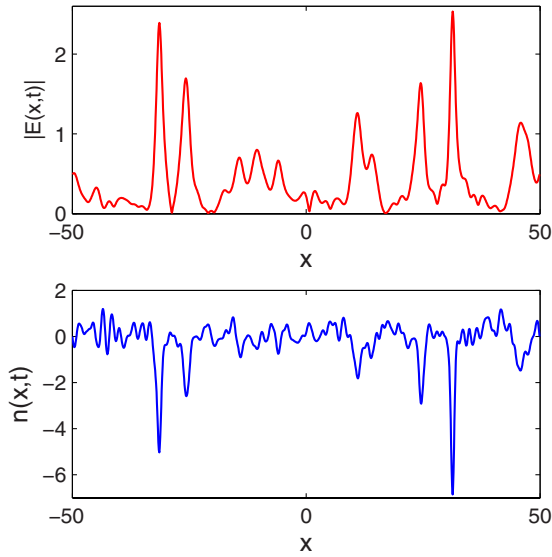


FIG. 1. (Color online) The profiles of the electric field [the red line (upper panel)] and the density fluctuations [blue line (lower panel)] for  $k=0.7$  and  $H=0$ . This shows the pattern selection in the process of the pattern formation. The positive-ion density perturbation is distributed among the patterns formed.

For  $k=0.7$  and  $H=0$ , many solitary pattern trains appear from the master mode and unstable harmonic modes [see Fig. 2]. In this case, solitons being strong can be seen after a long interval of time. The central stationary soliton, in particular, disappears right after a collision that sets it into a few oscillations. The stochastic motion of the trains leads to the collision between the neighboring coherent solitary patterns and fuse into a new incoherent pattern with the strengthened amplitude and the narrower width. At the same time, strong ion-acoustic wave emission is observed and the solitary patterns are seriously distorted. The occurrence of such an ion-acoustic wave emission due to the resonant interaction of central stationary soliton with the linear ion-acoustic waves

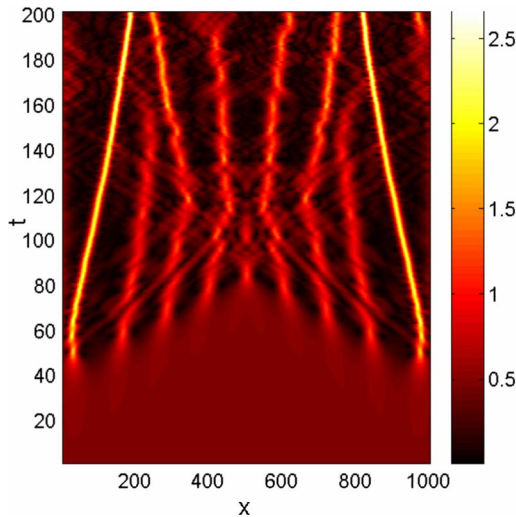


FIG. 2. (Color online) Contours of  $|E(x,t)|=const$  for the same values as in Fig. 1. This shows that many solitary pattern trains appear from the master mode and unstable harmonic modes.

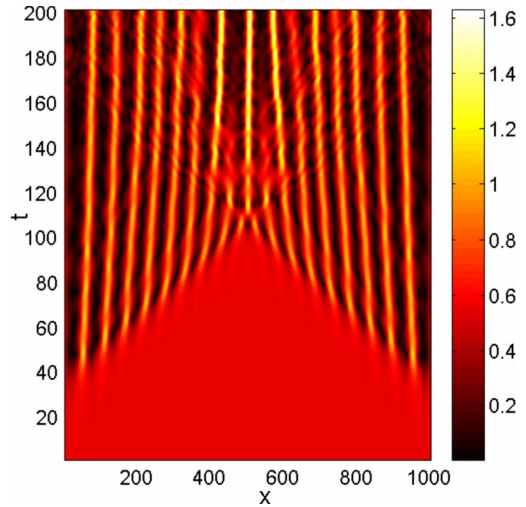


FIG. 3. (Color online) Contours of  $|E(x,t)|=const$  for  $k=0.7$  and  $H=0.5$ . This shows that at  $t \approx 110$ , two solitary patterns, initially peaked at  $x \approx 500$  and  $x \approx 700$ , collide and fuse into a new pattern with a strengthened amplitude and narrower width. At  $t \approx 150$ , other two patterns, initially peaked at  $x \approx 400$  and  $x \approx 650$ , collide with the master patterns at  $x \approx 350$  and  $x \approx 700$ , respectively, and then fuse into another new ones. The system is still in the coexistence of TC and STC.

propagating with the soliton Mach speed was observed by Karpman and Schamel [40] in the classical Zakharov system, where only the dispersive effects were considered due to particles' charge separation. In the quasineutral classical plasma (i.e., without the charge separation and quantum diffraction effects), since the linear sound modes propagate with the speed  $c_s = \sqrt{k_B T_e / m_i}$  greater than the soliton Mach speed, similar interaction of the Langmuir soliton with the sound wave may not be possible [40]. In quasineutral classical Zakharov system, strong ion-acoustic wave emission is possible due to stochastic motion of the center of the solitarylike patterns as observed in Fig. 2. In the quantum Zakharov system where only the dispersion is provided by the quantum diffraction effects, the collisions of the solitary patterns with the master one take place and then fuse into another new ones as can be seen from Fig. 3 below. For  $k=0.7$  and  $H=0.5$ , Fig. 3 shows that at  $t \approx 110$ , two solitary patterns, initially peaked at  $x \approx 500$  and  $x \approx 700$ , collide and fuse into a new pattern with a strengthened amplitude and narrower width. At  $t \approx 150$ , other two patterns, initially peaked at  $x \approx 400$  and  $x \approx 650$ , collide with the master patterns at  $x \approx 350$  and  $x \approx 700$ , respectively, and then fuse into another new ones. Note that after these collisions, new patterns produced by the four harmonic patterns are coexistent with the distorted master patterns.

Different feature can be observed for increasing the value of  $H=0.6$  and fixed  $k=0.7$  (see Fig. 4). Here at  $t \approx 120$ , three solitary patterns initially peaked at  $x \approx 450, 550,$  and  $650$  collide to form two new solitary patterns which again collide and fuse to form another new one with strengthened amplitude. Two other collisions can also be observed at  $t \approx 190$ . However, from the above observations we note that a few collisions do not seem to be enough to cause STC as can be seen from the spatial correlation function [37]. Thus, the co-

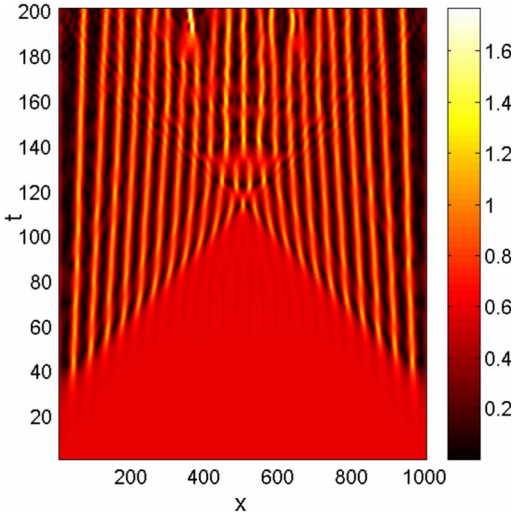


FIG. 4. (Color online) Contours of  $|E(x,t)|=\text{const}$  for  $k=0.7$ , but  $H=0.6$ . Different features can be observed (in comparison to Fig. 1). Here at  $t \approx 120$ , three solitary patterns initially peaked at  $x \approx 450, 550$ , and  $650$  collide to form two new solitary patterns which again collide and fuse to form another new one with strengthened amplitude. Two other collisions can also be seen at  $t \approx 190$ . The SPC state still exists in the system.

herence of the system is still retained so that SPC still exists in the system. If we now consider the case of increased  $H=0.7$  and  $k=0.7$ , many unstable modes are excited and saturated to form initially different many solitary patterns as can be seen from Fig. 5. Collisions and fusion among some trains take place soon and the new incoherent pattern trains are formed accompanying strong ion-acoustic emission. Then these incoherent patterns collide with others again and again after some time. Finally, a few solitary pattern trains are fused into a number of incoherent patterns in stochastic motion. A certain amount of the system energy is carried out by

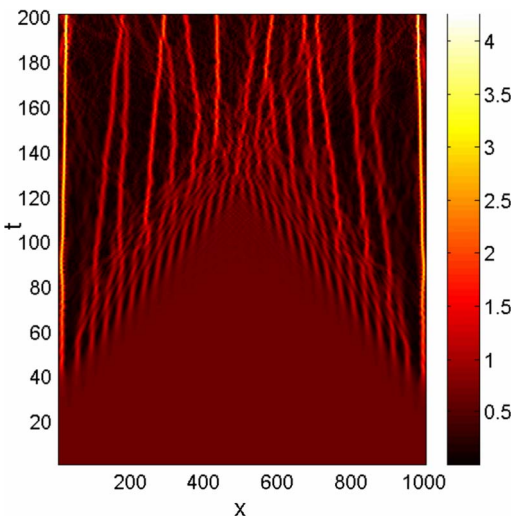


FIG. 5. (Color online) Contours of  $|E(x,t)|=\text{const}$  for  $k=0.7$  and  $H=0.7$ . Here many solitary patterns are formed. After some time collision and fusion among some trains take place and the new incoherent pattern trains are formed accompanying strong ion-acoustic emission; the STC state emerges.

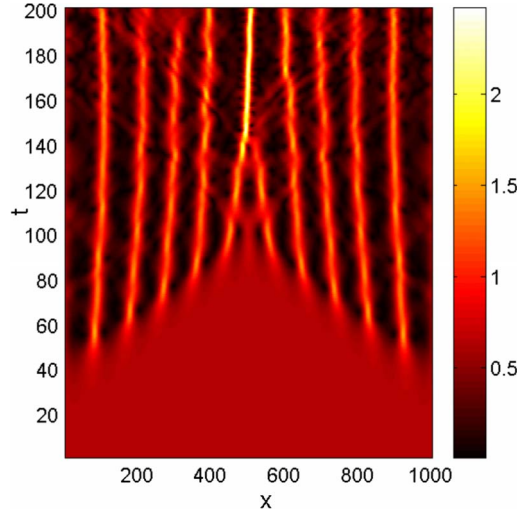


FIG. 6. (Color online) Contours of  $|E(x,t)|=\text{const}$  for  $k=0.9$  and  $H=0.0$ . Similar phenomena can be observed as in Fig. 2. This shows that two solitary patterns excited at  $x \approx 425$  and  $x \approx 620$  in time  $t=145$  collide and fuse to form another pattern, coexistent with master modes, with strengthened amplitude and narrower width.

the incoherent patterns, as well as many stable harmonic modes ( $\hat{k} > 1$ ) are excited through nonlinear interactions. The system energy in the STC state is thus spatially redistributed in the process of pattern collisions, fusion, and distortion. Hence, collisions and fusion of many pattern trains can lead to the existence of STC state, if initially there exist many unstable modulation lengths to form patterns. There should then exist critical values of both  $k$  and  $H$  where the transition from TC to STC can occur. Similar phenomena can also be well observed by considering the different values of  $k$  and  $H$ . As for example, for  $k=0.9$ ,  $H=0$ , Fig. 6 shows that two solitary patterns excited at  $x \approx 425$  and  $x \approx 620$  in time  $t=145$  collide and fuse to form another pattern, coexistent with master modes, with strengthened amplitude and narrower width. However, if we consider case of increased  $H \geq 0.4$  with  $k=0.9$ , we can observe many solitary patterns which after some time collide, fuse, and distort as can be seen from Fig. 7 for  $H=0.7$ ,  $k=0.9$ .

For the infinite-dimensional system, the adiabatic limit is obtained by disregarding the second-order time derivative of the density fluctuation in Eq. (2). The resulting equations then read

$$i \frac{\partial E}{\partial t} + \frac{\partial^2 E}{\partial x^2} + |E|^2 E = H^2 \left( \frac{\partial^4 E}{\partial x^4} + E \frac{\partial^2 n}{\partial x^2} \right), \quad (6)$$

$$H^2 \frac{\partial^2 n}{\partial x^2} - n = |E|^2. \quad (7)$$

In the formal classical limit  $H \rightarrow 0$ , Eq. (7) decouples becoming the familiar NLSE. In the quantum case, however, even the adiabatic limit shows a coupled nonlinear system, whose properties remains to be fully understood but beyond the scope of the present work. However, the system can be de-

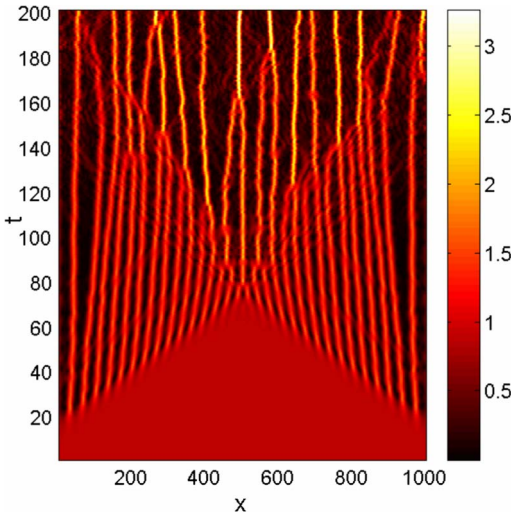


FIG. 7. (Color online) Contours of  $|E(x,t)|=\text{const}$  for  $k=0.9$ , but  $H=0.7$ . Many solitary patterns are formed, which after some time collide, fuse, and distort as in Fig. 5. The system is in STC.

coupled in the consideration of simultaneously semiclassical ( $H \ll 1$ ) as well as adiabatic limit as

$$i \frac{\partial E}{\partial t} + \frac{\partial^2 E}{\partial x^2} + |E|^2 E = H^2 \left( \frac{\partial^4 E}{\partial x^4} - E \frac{\partial^2 |E|^2}{\partial x^2} \right). \quad (8)$$

Equation (8) can be used to study perturbations of the classical nonlinear Schrödinger (NLS)–soliton solutions. The numerical solutions of Eq. (8) are presented in Fig. 8 for different values of  $H$ . These figures show the contour plots for  $|E(x,t)|$  for  $H=0$  and  $H=0.15$ . We observe that solitons can be identified during a large period of time. The central stationary soliton, which disappears in the classical case (see upper panel of Fig. 8), becomes strong in the semiclassical case ( $H=0.15$ , lower panel of Fig. 8). The pattern evolutions show that solitons are stronger in the semiclassical case, where the quantum coupling parameter is ultimately responsible for such existence of solitons. Thus, in contrast to the quantum Zakharov cases, the NLS solitons are virtually indestructible in classical as well as semiclassical cases.

### III. CONCLUSION

A simulation study of the quantum Zakharov system has been performed to show that many coherent solitary patterns can be excited and saturated via the MI of unstable harmonic modes excited by a modulation wave number of monoenergetic quantum Langmuir waves (QLWs). It is observed that there exist critical values of  $k$  and  $H$  for which the motion of the coherent solitary patterns is the temporal recurrence (periodic) or the pseudorecurrence (quasiperiodic) when the unstable wave number lies in  $0 < k < 0.9$  for  $H=0$  and that of the solitary pattern is STC when  $k \geq 0.9$  for  $H=0$  or for  $k \geq 0.7$ ,  $H \geq 0.5$ . If few harmonic patterns coexist with the master mode, the system will be in TC and SPC, and if many harmonic patterns occur in the early phase, the system may experience SPC state. Collisions and fusion among some

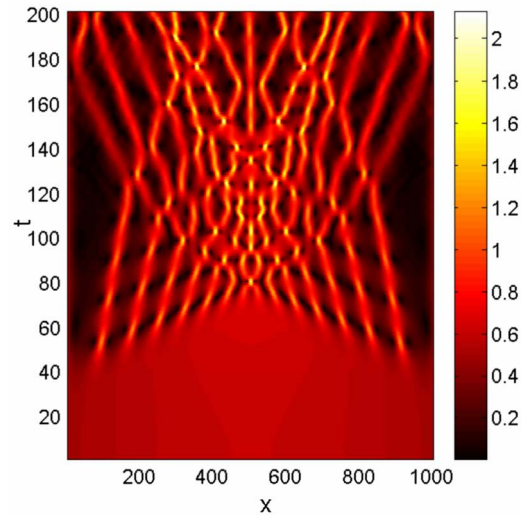
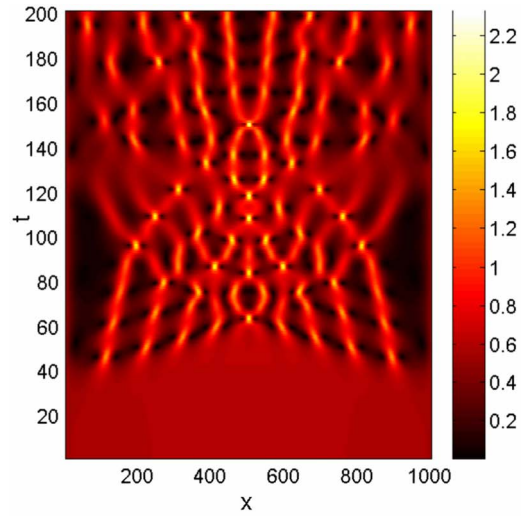


FIG. 8. (Color online) Contours of  $|E(x,t)|=\text{const}$  for  $H=0.0$  (upper panel) and for  $H=0.15$  (lower panel) [The numerical solutions of Eq. (25)]. Notice that solitons can be observed during a large period of time. The central stationary soliton, which disappears in the classical case (upper panel), becomes strong in the semiclassical case (lower panel).

trains take place and the new incoherent pattern trains are formed accompanying strong ion-acoustic wave emission; the STC state then emerges. As a result, the system energy in the STC state is spatially redistributed in the process of pattern collision, fusion, and distortion, which may switch on the onset of weak turbulence in quantum plasmas.

### ACKNOWLEDGMENTS

This work was partially supported by the Special Assistance Program (SAP), University Grants Commission (UGC), Government of India, through Sanction Letter No. F.510/8/DRS/2004 (SAP-I), as well as by the Partial Research Grant from Visva-Bharati University, Santiniketan, India.

- [1] P. A. Markowich, C. A. Ringhofer, and C. Schmeiser, *Semi-conductor Equations* (Springer-Verlag, New York, 1990).
- [2] K. H. Becker, K. H. Schoenbach, and J. G. Eden, *J. Phys. D* **39**, R55 (2006).
- [3] M. Opher, L. O. Silva, D. E. Dauger, V. K. Decyk, and J. M. Dawson, *Phys. Plasmas* **8**, 2454 (2001).
- [4] F. Haas, L. G. Garcia, J. Goedert, and G. Manfredi, *Phys. Plasmas* **10**, 3858 (2003).
- [5] F. Haas, *Phys. Plasmas* **12**, 062117 (2005).
- [6] P. K. Shukla and L. Stenflo, *New J. Phys.* **8**, 111 (2006).
- [7] F. Haas, *Europhys. Lett.* **77**, 45004 (2007).
- [8] A. P. Misra and C. Bhowmik, *Phys. Plasmas* **16**, 012103 (2009).
- [9] A. P. Misra and P. K. Shukla, *Phys. Plasmas* **15**, 122107 (2008).
- [10] A. P. Misra and S. Samanta, *Phys. Plasmas* **15**, 122307 (2008).
- [11] L. Stenflo, P. K. Shukla, and M. Marklund, *Europhys. Lett.* **74**, 844 (2006).
- [12] P. K. Shukla and L. Stenflo, *Phys. Lett. A* **355**, 378 (2006).
- [13] P. K. Shukla and L. Stenflo, *Phys. Plasmas* **13**, 044505 (2006).
- [14] P. K. Shukla and S. Ali, *Phys. Plasmas* **12**, 114502 (2005).
- [15] S. Ali and P. K. Shukla, *Phys. Plasmas* **13**, 022313 (2006).
- [16] A. P. Misra and A. R. Chowdhury, *Phys. Plasmas* **13**, 072305 (2006).
- [17] M. Marklund and G. Brodin, *Phys. Rev. Lett.* **98**, 025001 (2007).
- [18] G. Brodin, M. Marklund, J. Zamanian, A. Ericsson, and P. L. Mana, *Phys. Rev. Lett.* **101**, 245002 (2008).
- [19] P. K. Shukla, *Nat. Phys.* **5**, 92 (2009).
- [20] G. Brodin and M. Marklund, *Phys. Rev. E* **76**, 055403(R) (2007).
- [21] S. H. Glenzer, O. L. Landen, P. Neumayer, R. W. Lee, K. Widmann, S. W. Pollaine, and R. J. Wallace, *Phys. Rev. Lett.* **98**, 065002 (2007).
- [22] P. K. Shukla and B. Eliasson, *Phys. Rev. Lett.* **96**, 245001 (2006).
- [23] D. Shaikh and P. K. Shukla, *Phys. Rev. Lett.* **99**, 125002 (2007).
- [24] D. Shaikh and P. K. Shukla, *New J. Phys.* **10**, 083007 (2008).
- [25] G. Manfredi, *Fields Inst. Commun.* **46**, 263 (2005).
- [26] L. G. Garcia, F. Haas, J. Goedert, and L. P. L. Oliveira, *Phys. Plasmas* **12**, 012302 (2005).
- [27] V. E. Zakharov, *Sov. Phys. JETP* **35**, 908 (1972).
- [28] M. Marklund, *Phys. Plasmas* **12**, 082110 (2005).
- [29] F. Haas, *Phys. Plasmas* **14**, 042309 (2007).
- [30] A. P. Misra, D. Ghosh, and A. R. Chowdhury, *Phys. Lett. A* **372**, 1469 (2008).
- [31] R. P. Sharma, K. Batra, and A. D. Verga, *Phys. Plasmas* **12**, 022311 (2005).
- [32] K. Batra, R. P. Sharma, and A. D. Verga, *J. Plasma Phys.* **72**, 671 (2006).
- [33] M. C. Cross and P. C. Hohenberg, *Rev. Mod. Phys.* **65**, 851 (1993).
- [34] X. T. He and C. Y. Zheng, *Phys. Rev. Lett.* **74**, 78 (1995).
- [35] F. B. Rizzato, G. I. deOliveira, and R. Erichsen, *Phys. Rev. E* **57**, 2776 (1998).
- [36] X. T. He, C. Y. Zheng, and S. P. Zhu, *Physica A* **288**, 338 (2000).
- [37] X. T. He, C. Y. Zheng, and S. P. Zhu, *Phys. Rev. E* **66**, 037201 (2002).
- [38] F. B. Rizzato, G. I. deOliveira, and A. C.-L. Chian, *Phys. Rev. E* **67**, 047601 (2003).
- [39] Y. Tan, X. T. He, S. G. Chen, and Y. Yang, *Phys. Rev. A* **45**, 6109 (1992).
- [40] V. I. Karpman and H. Schamel, *Phys. Plasmas* **4**, 120 (1997).